scientific reports

OPEN

Development of an advanced multimode refractive index plasmonic optical sensor utilizing split ring resonators for brain cancer cell detection

Ali Khodaie[1], Hamid Heidarzadeh[1]✉ & Farrokhfar Valizadeh Harzand[2]

In this paper, we propose and theoretically investigate a novel multimode refractive index (MMRI) plasmonic optical sensor for detecting various brain cancer cells, leveraging the unique capabilities of split ring resonators (SRRs). The sensor, simulated using the finite-difference time-domain (FDTD) method, exhibits dual resonance modes in its reflection spectrum within the 1500 nm to 3500 nm wavelength range, marking a significant advancement in multimode plasmonic biosensing. Through detailed parametric analysis, we optimize critical dimensional parameters to achieve superior performance. The novelty of this work lies in the dual-mode sensing mechanism, which enables robust detection by exploiting the resonance characteristics of gold, silver, and aluminum. These materials provide tunable and highly sensitive interactions with light, enhancing the sensor's adaptability for a wide range of applications. The results reveal exceptional sensitivity values of 1778.3 nm/RIU, a limit of detection (LOD) of 0.016 RIU, and a high figure of merit (FOM) of 7 RIU^{-1}, along with a quality factor (QF) of 11.7 in the first resonance mode. The findings show that the designed optical biosensor exhibits high sensitivity, a good LOD, and an acceptable FOM in both resonance modes. So, this work paves the way for future research and development of susceptible, multimode optical sensors for medical diagnostics. The results indicate that the proposed sensor operates effectively across a range of temperatures and angles of radiant light, demonstrating its independence from these variables. This reliability in performance underscores its potential for use in diverse environments, making it a dependable tool for detecting biological samples, including brain cancer cells, irrespective of external conditions.

Keywords Optical sensor, High sensitivity, Brain cancer cells, Multimode refractive index (MMRI), Split ring resonator (SRR)

The field of optical sensing has seen remarkable advancements over the past few decades, driven by the need for highly sensitive, selective, and non-invasive diagnostic tools[1]. Optical biosensors, in particular, have emerged as promising candidates in biomedical applications due to their capability to detect subtle biological and chemical changes with high accuracy. Among the various types of optical biosensors, plasmonic sensors have garnered significant attention due to their ability to exploit the interaction of light with metallic nanostructures, leading to surface plasmon resonance (SPR) effects[2]. These effects are highly sensitive to changes in the refractive index of the surrounding medium, making plasmonic sensors ideal for applications in medical diagnostics, environmental monitoring, and biochemical analysis[3]. A critical area where this technology holds immense potential is in the detection and diagnosis of brain lesions[4]. Brain lesions are areas of damaged tissue within the brain that can be caused by a variety of conditions, including traumatic injury, stroke, infections, and tumors. These lesions can present as areas of inflammation, degeneration, or necrosis and can vary greatly in size, location, and severity. Their detection, accurate characterization, and monitoring are of paramount importance, especially in conditions like brain cancer, multiple sclerosis, or traumatic brain injuries (TBI)[5,6]. Brain lesions come in many forms, including neoplastic (tumors), ischemic (stroke-related), demyelinating (such as those

[1]Department of Electrical and Computer Engineering, University of Mohaghegh Ardabili, Ardabil, Iran. [2]Department of Chemical Engineering, University of Mohaghegh Ardabili, Ardabil, Iran. ✉email: heidarzadeh@uma.ac.ir

seen in multiple sclerosis), and infectious (such as abscesses). Each type presents unique challenges for medical professionals in terms of detection, diagnosis, and treatment. Tumors, for instance, can grow slowly and remain asymptomatic for a long time, only becoming noticeable when they press on critical areas of the brain. In contrast, ischemic lesions caused by strokes or traumatic injuries can have sudden, devastating effects, leading to motor and cognitive impairments[7,8].

Traditional imaging techniques such as magnetic resonance imaging (MRI) and computed tomography (CT) scans are the gold standards for diagnosing brain lesions. These techniques offer detailed structural images of the brain, allowing clinicians to locate lesions, estimate their size, and sometimes differentiate between lesion types based on imaging characteristics[9]. However, despite their usefulness, these methods have limitations. MRI and CT often require expensive, bulky equipment and are generally used in clinical or hospital settings, making them less accessible for real-time monitoring. Furthermore, these techniques may not always offer the sensitivity required to detect early-stage lesions or subtle changes in lesion size and composition, which are crucial for conditions such as cancer or multiple sclerosis where early intervention can significantly improve outcomes[10]. Moreover, MRI and CT scans are often limited by their inability to provide continuous, real-time monitoring. This can be particularly problematic in cases of traumatic brain injury (TBI), where the patient's condition may change rapidly over time. For example, in the acute phase after a head injury, brain swelling or bleeding may not be immediately visible on an initial scan but can progress to life-threatening levels within hours or days. As such, a diagnostic tool that offers higher sensitivity, real-time monitoring, and a non-invasive approach could significantly improve outcomes in managing brain lesions[11]. Membrane technologies, primarily utilizing conventional polymers, represent the most widely used commercial approaches for environmental remediation involving air, water, solids, and radiation. However, these polymeric membranes face significant challenges such as low stability at elevated temperatures, swelling in the presence of organic pollutants, and inadequate selectivity, which hinder their scalability[12]. Too, metal/metal oxide nanosystems (M-NSs), characterized by adjustable and controllable properties, are gaining traction in cancer management through advancements in immunotherapy, early detection, nanotherapeutics, and targeted drug delivery systems. Nevertheless, their widespread adoption is constrained by concerns over significant toxicity, non-targeted effects, insufficient biocompatibility, and high costs[13]. To address these limitations, there is growing interest in alternative diagnostic technologies, particularly those based on optical sensing. Sensors play a crucial role in tracking the release of different gases and volatile organic pollutants from various human activities, as well as in detecting environmental pathogens[14]. Biosensors utilizing nanomaterials have become cost-effective, efficient, selective, rapid, and precise methods for detecting pathogens[15]. The core detection mechanism is based on the interaction between respiratory biomarkers and sensors, leading to changes in essential optical properties, including surface plasmon resonance, fluorescence, reflectance, absorption, emission, phosphorescence, and refractive index[16]. Optical biosensors have the potential to detect changes at the molecular level, offering much higher sensitivity compared to conventional imaging techniques. One of the most promising types of optical biosensors is the plasmonic sensor, which leverages the interaction of light with metallic nanostructures to detect minute changes in the surrounding environment's refractive index[17]. Brain lesions, which alter the composition and refractive index of the affected brain tissue, are ideal targets for such sensors. For instance, cancerous tissues often have a different refractive index compared to healthy tissue due to the high rate of cellular growth and the accumulation of biological markers like proteins and DNA. Similarly, inflammatory lesions, common in conditions like multiple sclerosis, can cause localized swelling and changes in tissue composition, leading to detectable shifts in the refractive index. This makes optical sensors particularly suited to identifying and characterizing such lesions in a non-invasive manner[18].

In the context of brain lesion detection, SRR-based plasmonic sensors have several key advantages over traditional methods. First, they offer a much higher sensitivity to refractive index changes, allowing for the detection of even the smallest lesions that might be missed by MRI or CT scans[17]. This is particularly important for early diagnosis, where detecting a lesion at its earliest stage can lead to better treatment outcomes. Second, the multimode resonance capability of SRRs enables the sensor to operate across a range of wavelengths, providing multiple detection channels and improving accuracy in identifying different types of lesions. Another significant advantage of plasmonic sensors is their potential for real-time monitoring. Unlike MRI or CT, which require patients to be moved into a scanning machine, plasmonic sensors could be developed into portable or even implantable devices that continuously monitor changes in brain tissue. This would be particularly beneficial in monitoring the progression of brain lesions in conditions like multiple sclerosis, where lesion activity fluctuates over time, or in patients with traumatic brain injuries who require close observation for potential secondary damage[19]. SRR-based plasmonic sensors offer the potential for integration with other medical technologies, such as wearable devices or smart implants. By providing continuous data on brain lesion activity, these sensors could enable personalized treatment approaches, where therapies are adjusted in real-time based on the progression of the disease. This could be transformative for conditions like brain cancer, where timely adjustments to treatment plans can significantly affect patient outcomes[20]. Figure 1 shows the application and potential of the plasmonic optical sensor for the diagnosis of brain lesions. Here, we didn't used any tissues. The proposed sensor is evaluated in a simulated environment to model the optical properties of brain lesion tissues. The simulation accurately represents the refractive index of the lesion tissue, a critical parameter that governs how light interacts with and refracts through the material. By leveraging these virtual models, the study provides insights into the sensor's performance without the need for physical tissue samples. This approach enables detailed analysis of light-tissue interactions, offering a pathway to optimize the sensor for potential diagnostic applications in neurology, particularly in the detection and characterization of brain lesions.

In this study, we present a theoretical investigation of a multimode refractive index (MMRI) plasmonic optical sensor based on SRR structures for the detection of brain lesions. The proposed sensor is designed to operate within the near-infrared (NIR) range, which is known for its deep tissue penetration and minimal absorption in biological tissues, making it ideal for medical diagnostics. The sensor's design leverages the unique resonance

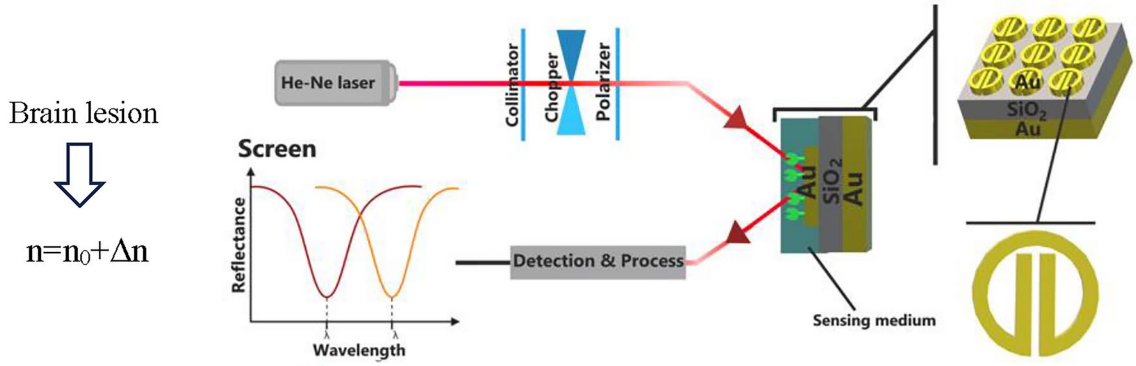

Fig. 1. Application and operation mode of the proposed sensor in the diagnosis of brain lesions.

properties of SRRs, which support multiple resonant modes, thereby increasing the range and sensitivity of detection. By optimizing the geometrical and material parameters of the SRRs, we aim to achieve a sensor with high sensitivity, a high figure of merit (FOM), and excellent resolution for detecting changes in the refractive index associated with brain lesions. Using the finite-difference time-domain (FDTD) method, we simulate the interaction between light and the plasmonic sensor to analyze its performance. The simulation covers a wide range of wavelengths from 1500 to 3500 nm, where the sensor exhibits two distinct resonance modes. These modes allow for the precise detection of refractive index changes in the surrounding medium, which can be attributed to the presence of biological tissues or abnormalities such as brain lesions. The results of our analysis show that the proposed sensor is capable of detecting brain lesions with a high sensitivity of up to 1778 nm/RIU, making it a promising tool for biomedical diagnostics. In last years other materials like MXenes have been used in plasmonic biosensors. MXenes exhibit high potential as materials for plasmonic optical sensor applications. Their unique combination of metallic conductivity, tunable surface chemistry, and high optical transparency makes them highly promising for significantly enhancing the performance of plasmonic sensors[21]. Their two-dimensional structure enables strong light-matter interaction, which could improve the sensitivity and efficiency of sensors based on split ring resonators (SRRs). Furthermore, the chemical stability and compatibility of MXenes with biological environments make them ideal for applications such as detecting cancerous tissues, monitoring glucose levels, and identifying pathogenic microorganisms. Future studies could investigate the integration of MXenes into the proposed sensor design to unlock new capabilities and expand its application scope[22]. Furthermore, it is suggested to explore the broader potential applications of the sensor beyond brain lesion detection, such as its possible use in detecting cancerous tissues, monitoring glucose levels, and identifying pathogenic microorganisms. The versatility of the SRR-based plasmonic sensor, combined with its multimode detection capabilities, positions it as a cutting-edge technology in the realm of biosensing. In conclusion, the development of an SRR-based multimode refractive index plasmonic sensor offers a novel approach to enhancing the sensitivity and accuracy of optical biosensors for medical applications. The ability to detect brain lesions with high precision in a non-invasive manner represents a significant advancement in medical diagnostics, providing a new tool for early diagnosis and real-time monitoring of neurological conditions. As this technology continues to evolve, it holds great promise for revolutionizing the way we approach disease detection and treatment in the future.

Structure and methodology
Background and materials
The simple design and effective performance of split ring resonator (SRR) structures have motivated researchers and engineers to further explore this type of sensor. The performance of the designed structure relies on the binding of chemical molecules or biological samples to the sensor's surface, which alters the effective refractive index of the local dielectric environment and subsequently affects the surface plasmon resonance frequency. SRR sensors are typically constructed from plasmonic metamaterials, which exhibit remarkable properties such as electrical conductivity and negative magnetic permeability. Gold, silver, and aluminum are recognized as prominent metamaterials and are utilized in the analysis of our proposed structure. Additionally, a layer of SiO_2 acts as the dielectric substrate. For optimal performance, we selected a layer of gold, silver, and aluminum as the reflective backing layer. The refractive indices of gold, silver, aluminum, and SiO_2 were obtained from Edward D. Palik's handbook on optical constants of solids[23]. Furthermore, the refractive indices of brain cancer cells are presented in Table 1, as measuring them is one of the primary objectives of this research.

Design mechanism
The structure of the multimode plasmonic refractive index optical sensor based on the Split Ring Resonator (SRR) is illustrated from different perspectives in Fig. 2. The proposed structure consists of a ring resonator with inner and outer radii, denoted as R_{in} and R_{out}, respectively, and a ring width $W_r = R_{out} - R_{in}$. Additionally, an air gap with length g is introduced in the ring resonator. Moreover, two parallel arms are positioned inside the ring resonator, each with width W_r and length d, separated by a distance g. The thickness of the ring and the arms are defined as h_r, and after material optimization, the ring resonator and arms are made of gold.

Refractive index (n)	Brain tissues
1.3333	CSF
1.3531	Oligodendroglioma
1.3951	Gray matter
1.4320	Low-grade glioma
1.4591	Lymphoma
1.4833	Metastasis

Table 1. Refraction coefficients of different brain lesions[24].

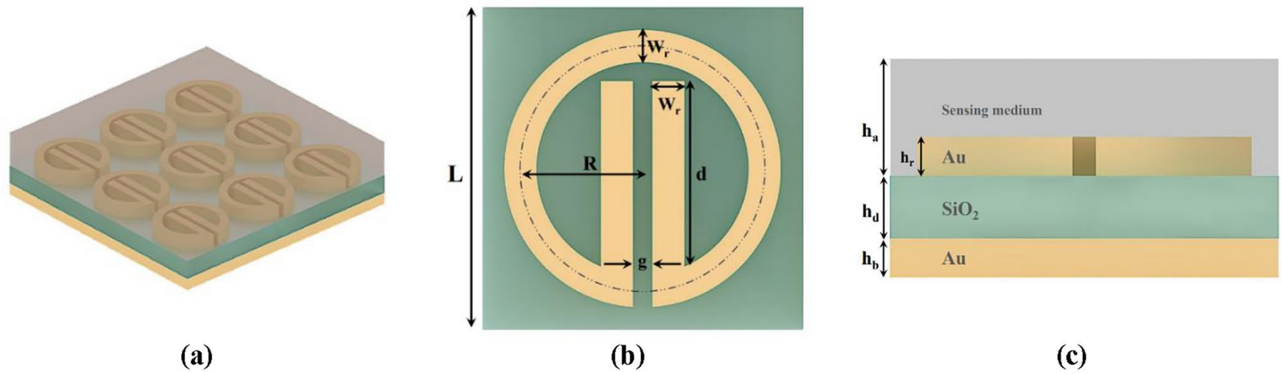

Fig. 2. The proposed optical sensor configuration from, (**a**) 3D, (**b**) top, and (**c**) front views.

Parameter	Symbol	Value (nm)
Structure simulation period	L	1000
Air gap length	g	60
The radius of the ring	R	380
Ring width	W_r	100
Arms length	d	600
Back reflector thickness	h_b	100
Dielectric thickness	h_d	160
Rings thickness	h_r	110
Analyte thickness	h_a	300

Table 2. Geometrical parameters of the proposed optical sensor after dimension optimization.

The ring resonators and arms are embedded on a dielectric substrate made of SiO_2 with a thickness of h_d. A backing layer with thickness h_b acts as the reflective backing, and an array of SRRs with a periodicity of *L* is modeled. The geometrical parameters of the proposed structure after optimization are detailed in Table 2. Various fabrication techniques for SRRs, including stress-driven curving, Computer Numerical Control (CNC) machining, nanoimprint lithography, and etching, are available[25,26]. Pre-fabrication simulations of plasmonic structures are beneficial for several reasons[27]. By modeling the geometry of the structure, researchers can evaluate material properties and excitation conditions, allowing them to optimize the design and predict performance characteristics. This simulation process aids in making informed decisions regarding fabrication. The fabrication and real-world implementation of the proposed plasmonic optical sensor utilizing split ring resonators (SRRs) presents several practical challenges that must be addressed to make the design feasible for practical applications. One of the primary challenges is the precision required in fabricating SRRs at the nanoscale. Achieving such fine geometries necessitates the use of advanced fabrication techniques like electron-beam lithography or focused ion beam milling. These methods, while highly precise, are often time-consuming and costly, making them less practical for large-scale production. Additionally, ensuring uniformity and reproducibility of SRRs over a large area is a significant hurdle, especially when scaling up for industrial production[28]. Material selection poses another critical challenge. The materials used for SRRs need to exhibit stable optical and mechanical properties while minimizing losses in the plasmonic regime. This requirement limits the choice of materials and can further complicate the fabrication process[29]. Moreover, the integration of the sensor into clinical diagnostic systems requires the development of compatible interfaces. Aligning and packaging the sensor to maintain high sensitivity and accuracy in real-world conditions is another critical concern that demands innovative engineering solutions. Furthermore, the sensor's performance in biological environments introduces additional complexities. Factors such as pH variations, temperature changes, and biofouling can significantly affect the sensor's reliability and accuracy. Addressing these issues may involve designing protective coatings or developing calibration techniques to compensate for environmental effects. By considering and addressing these practical challenges, the research can provide a more realistic pathway toward the eventual implementation of this advanced sensor in clinical and industrial settings.

Analysis method

The proposed structure is simulated using the finite-difference time-domain (FDTD) method to solve Maxwell's equations. In the FDTD setup, an automatic non-uniform mesh is defined, and the Conformal0 type is selected to enhance mesh quality. The mesh accuracy is configured to "4," and for sensitive areas, an additional mesh with element size dx = dy = dz = 0.01 nm is implemented to ensure efficient simulation execution and sufficient accuracy for converged responses. The background refractive index of the simulation region is set to the refractive index of air, which is 1. The simulation duration is set at 300 K for 1000 fs using a Field time monitor. Perfectly matched layer (PML) boundary conditions are applied along the z-axis, while periodic boundary conditions are used along the x and y axes. A plane wave source emits light at wavelengths ranging from 1500 to 3500 nm with a polarization angle of 0 degrees. Additionally, a frequency domain field and power monitor are used to analyze the reflection spectrum, while a frequency domain field profile monitor evaluates the electromagnetic field distribution. A sample layer is placed on the structure to assess performance parameters, and by varying its refractive index (Δn_s), the changes in the surface plasmon resonance frequency ($\Delta\lambda_0$) are measured. As a result, the sensor sensitivity can be defined by the following equation[30]:

$$S = \frac{\Delta\lambda_0}{\Delta n_s} \tag{1}$$

It is important to note that relying solely on sensor sensitivity does not adequately capture the changes in the plasmonic spectrum, making it challenging to evaluate and compare sensor performance in terms of wavelength and energy. To address this issue, an additional parameter known as the figure of merit (FOM) is introduced, which is defined by the following equation[31]:

$$FOM = \frac{S}{FWHM} \tag{2}$$

where FWHM refers to the full width at half maximum.

Another criterion for evaluating the sensor's performance is the quality factor (QF). The QF of the sensor is defined as follows[32]:

$$QF = \frac{\lambda_0}{FWHM} \tag{3}$$

Additionally, the minimum measurable quantity that the sensor can detect is referred to as the limit of detection (LoD), which is defined as follows[17]:

$$LoD = \left(\frac{\Delta n_s}{1.5}\right) \times \left(\frac{FWHM}{\Delta\lambda_0}\right)^{1.25} \tag{4}$$

Results and discussion

Optimization of structural materials

The development of an effective platform for detecting brain cancer cells with enhanced sensitivity is described in this section. Initially, this study presents the reflection spectrum of the simulated structure based on a periodic arrangement of unit cells for the array of split ring resonators (SRRs). The findings indicate that the reflection spectrum exhibits two distinct resonance modes within the wavelength range of 1500 to 3500 nm. To evaluate the optimal sensor performance regarding surface plasmon resonance in these two modes, assessments are conducted using gold, silver, and aluminum as materials for the backing reflector. In the analysis of the split ring resonators (SRRs), the SRR configuration is first tested with gold, followed by silver, and then aluminum. As illustrated in Fig. 3a, b, when comparing the materials gold, silver, and aluminum for the SRRs, minimal changes in the reflection spectrum are observed for both resonance modes. The next step involves examining the sensitivity for both resonance modes, again utilizing gold, silver, and aluminum for both the backing reflector and SRRs. The results obtained in Fig. 3c, d demonstrate that gold exhibits slightly superior sensor performance in terms of sensitivity for both configurations (back reflector and SRR). Therefore, gold is ultimately selected as the metamaterial for the backing reflector and SRR to achieve optimal sensor performance in all modes.

Geometry optimization of the structure

After evaluating the materials used, the geometry of the sensor structure is examined to enhance its performance. Initially, the reflection spectrum is assessed for variations in the thickness of the backing reflector (h_b), and this process continues for changes in the thickness of the dielectric (h_d) and the ring resonator (h_r). As indicated in Fig. 4a–c, the investigations show that there is little variation in the sensor's reflection spectrum when altering

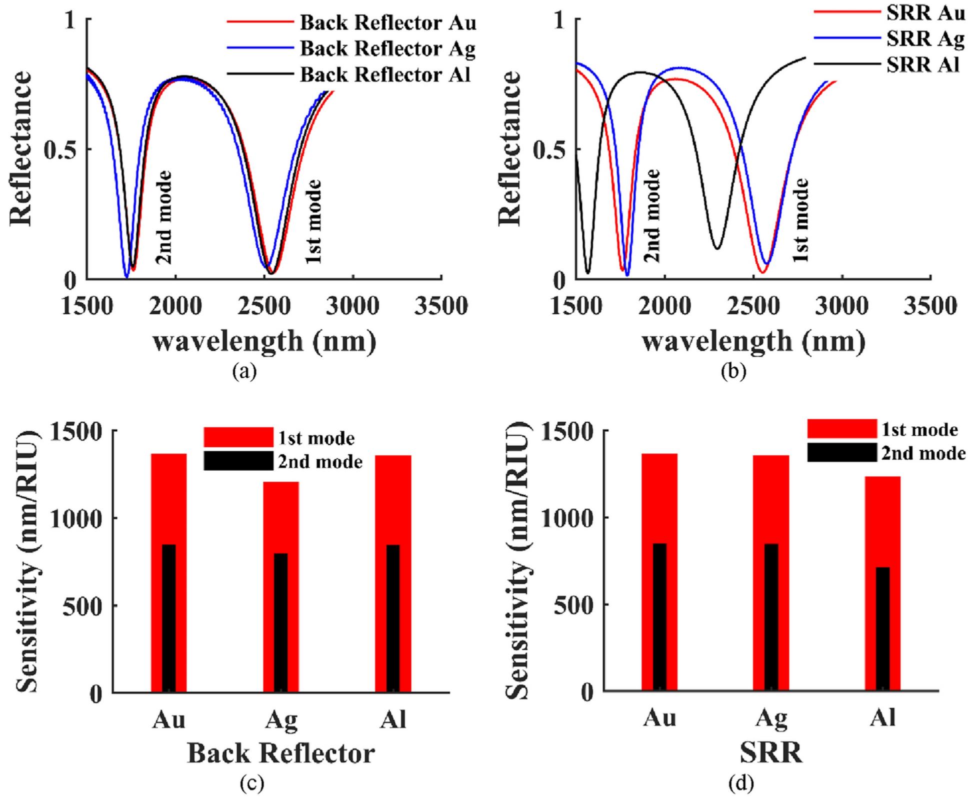

Fig. 3. (**a**,**b**) Reflectance spectrum of the proposed structure for gold, silver, and aluminum materials for back reflector and SRR, (**c**,**d**) comparison of sensor sensitivity in both resonance modes for gold, silver, and aluminum materials for back reflector and SRR.

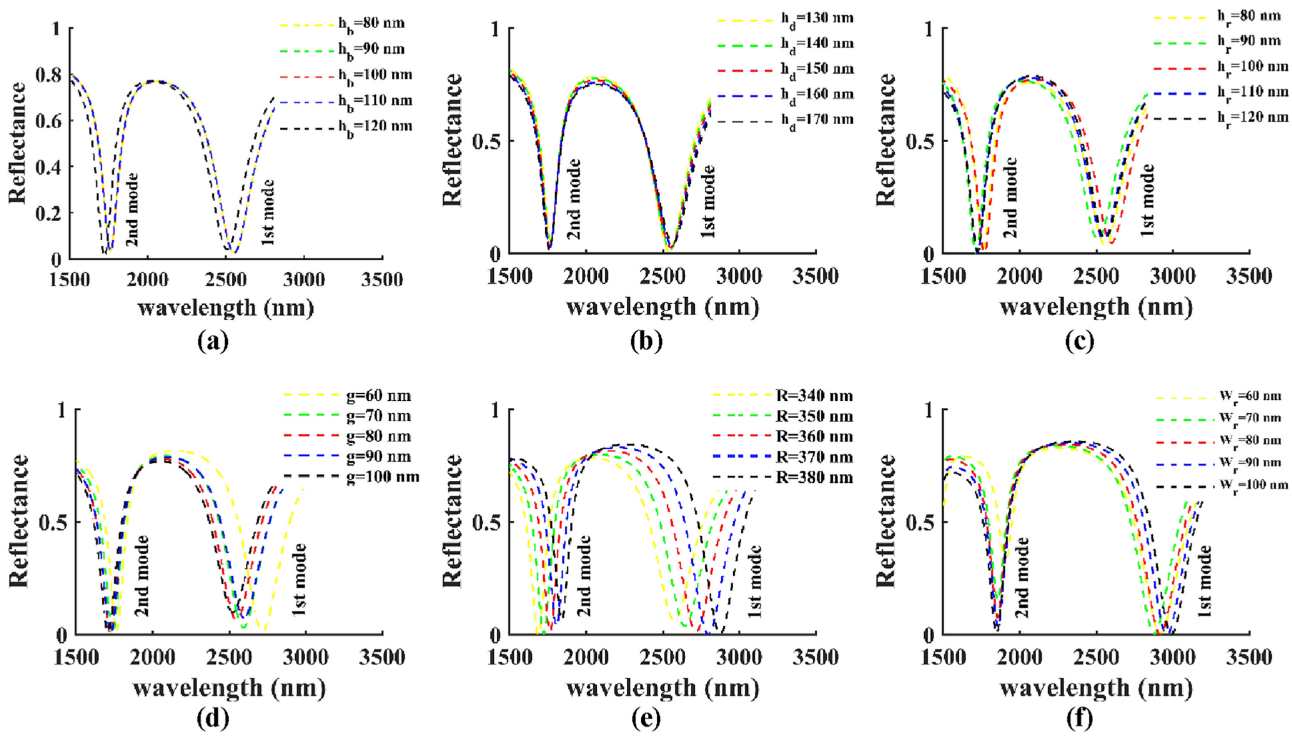

Fig. 4. The reflectance spectrum of the structure for changes in geometrical parameters, (**a**) h_b, (**b**) h_d, (**c**) h_r, (**d**) g, (**e**) R, and (**f**) W_r.

these three parameters. Subsequently, the reflection spectrum of the structure is examined using variations in the length of the air gap (g), the radius of the ring resonator (R), and the width of the ring resonator (W_r). As observed in Figs. 4d, f, changes in the parameters g and W_r do not significantly affect the second resonance mode, whereas, in the first mode, minor resonance shifts occur in the reflection spectrum. Additionally, according to Fig. 4e, altering the radius (R) of the SRRs causes the reflection spectrum curve to shift linearly in both resonance modes. Consequently, the geometry of the structure is further analyzed to optimize the sensor's sensitivity. Figure 5a–c demonstrate a linear increase in sensitivity for both resonance modes corresponding to increases in the dimensional parameters h_b, h_d, and h_r. Furthermore, as shown in Fig. 5e, f, increasing the radius and width of the ring resonators also optimizes the proposed sensor's sensitivity linearly; while the analyses presented in Fig. 5d indicate that increasing the length of the air gap results in a linear decrease in the structure's sensitivity. These investigations reveal an approximately linear relationship between sensitivity and these dimensions. The structural dimensions are examined to facilitate efficient simulation without issues related to time or convergence, as well as to ensure optimal sensor performance. Therefore, based on the criteria for optimal sensor performance and considering the limitations of the simulations, the optimal dimensions for the proposed sensor are determined.

Overall performance analysis of the structure

After optimizing the geometry of the structure, the overall sensitivity of the sensor system in both resonance modes is reassessed. The reflection spectrum of the sensor, illustrating the response of a test sample to changes in refractive index from $n = 1.33$ to $n = 1.49$, is presented in Fig. 6a. Figure 6b shows a linear plot with curve fitting, demonstrating how the resonance wavelength shifts in response to changes in refractive index for both resonance modes, with each line corresponding to a specific mode. The slope of these lines indicates the sensor's sensitivity for each resonance mode. The first mode exhibits the steepest slope, meaning that the sensor has the highest sensitivity in this mode, quantified at 1778.3 nm/RIU (with its linear equation represented as $y = 1788.3 \cdot x - 0.48889$). This sensor shows exceptional sensitivity in the first resonance mode, highlighting its potential for various applications in medical science, particularly for rapid detection of different brain cancer cells. Too the second resonance mode, demonstrating impressive performance metrics with a sensitivity of 995 nm/RIU, has the potential to assess additional diseases beyond the sensor's primary function of measuring brain lesions with the first mode. This capability enhances the sensor's versatility and broadens its range of potential applications. Additionally, this structure can function as a tunable frequency filters. In comparison to previously reported studies, the proposed sensor demonstrates improved sensitivity along with a more favorable FoM and QF. Additionally, the LoD for the presented structure has been calculated, an aspect that has received less attention in prior research. Furthermore, the sensor supports two resonance modes, each capable of serving distinct functions and applications, whereas most earlier works focus on single-resonance systems. Table 3 provides a comparison of this sensor's performance metrics with those from previous studies.

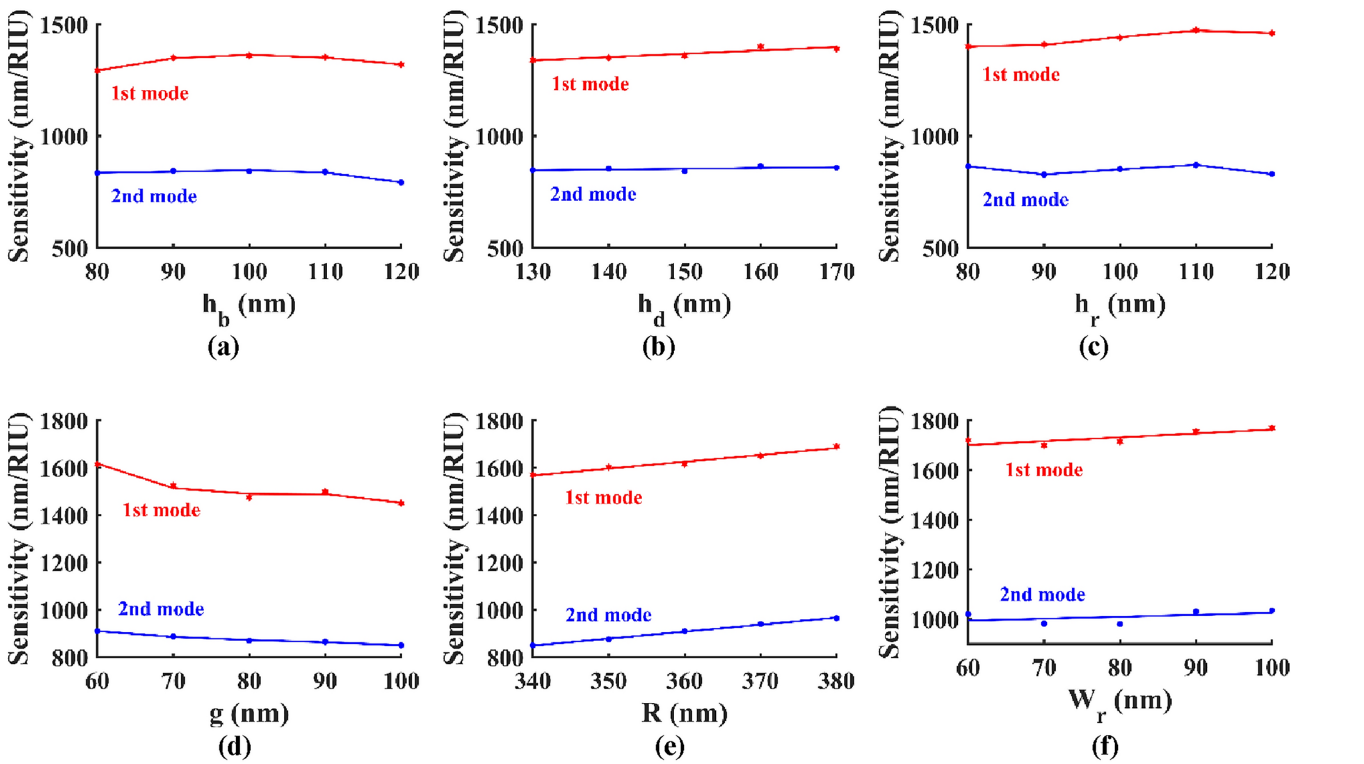

Fig. 5. Comparison of sensor sensitivity in both resonance modes for changes in geometrical parameters, (**a**) h_b, (b) h_d, (**c**) h_r, (**d**) g, (**e**) R, and (**f**) W_r.

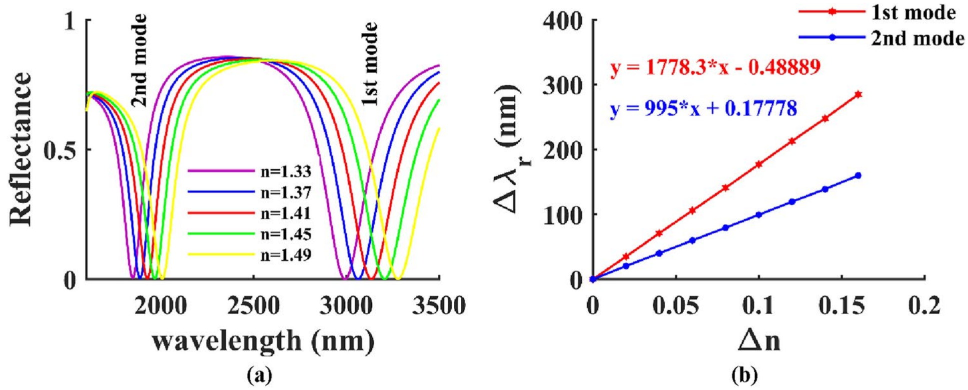

Fig. 6. (**a**) The reflectance spectrum of the proposed sensor for refractive index changes from n = 1.33 to n = 1.49 in order to check the overall performance of the structure and, (**b**) resonance wavelength changes versus refractive index changes in both resonance modes in the form of curve fitting.

References	Topology	Detection application	Sensitivity (nm/RIU)	FWHM (nm)	FOM (RIU^{-1})	QF	LoD
[34]	HSR	General	840	–	–	–	–
[35]	Three coupled HCs	General	1050	–	–	–	–
[36]	coupled nano-rings	cancer	524.3	52.3	10	–	–
[37]	SRR	Cancer cell	570.4	139.22	4.1	15.3	–
[38]	Hybrid Plasmonic Substrates	IgG	553	–	–	–	–
[39]	nano-particles	glucose/fructose	584.9	52	11.22	–	–
[40]	8-shaped resonator	Basal cancer cells	1200	–	–	–	–
[41]	Double Nanodisk Resonators	General	800	13	61.55		
This work (1st mode)	SRR	Brain lesions	1778.3	254.9	7	11.7	0.016
This work (2nd mode)	SRR	Other pathogens	995	117.25	8.5	15.7	0.017

Table 3. A comparison of the performance of the proposed sensor with previous works.

To further examine the designed structure, an analysis of the electromagnetic field response from a top view in both resonance modes is conducted. In the first mode, the electric field is primarily concentrated around the air gap of the SRR and the inner edges of the two parallel arms, while the magnetic field is distributed along the inner wall and within the two parallel arms. In the second mode, most of the electric field is located at the outer and terminal edges of the two parallel arms. Similarly, in the second mode, the magnetic field occupies the air gap, the space between the ring resonator and the ends of the two parallel arms, as well as the outer walls of the ring resonator along the x-axis. Figure 7a–d illustrate these findings regarding the electromagnetic field responses in both resonance modes.

Application of the sensor for brain cancer cell detection

In the United States, brain cancer cells pose a critical health issue, affecting nearly 700,000 individuals, with approximately 86,970 new diagnoses in 2019. These tumors are often lethal and significantly diminish the quality of life for patients. Classifying brain lesions based on their refractive indices is significant. Lesions with a refractive index lower than 1.395, such as those found in multiple sclerosis (1.3425) or certain brain abscesses (1.341), are considered benign. Conversely, lesions with a refractive index greater than 1.412 are classified as malignant, indicating a direct correlation between malignancy and their refractive indices[33]. Pure water has a refractive index of 1.33 and serves as an external reference point when evaluating cerebrospinal lesions as an internal reference. According to Gladstone-Dale's law, the refractive index of brain lesions is directly related to the density of proteins and lipids present, while exhibiting an inverse relationship with water content in the tissue. This relationship underscores the importance of understanding the physical properties of brain lesions in determining their nature and potential impact on patient health[24]. In Fig. 8a, the reflection spectrum of the structure in the first resonance mode, which shows the highest sensitivity, is presented for various refractive index values of brain cancer cells. Changes in the surface plasmon frequency are clearly observable. Figure 8b displays a linear plot with curve fitting, illustrating how the resonance wavelength shifts in response to changes in refractive index. As previously mentioned, the slope of these lines indicates the sensor's sensitivity in both resonance modes. The first mode exhibits the steepest slope or highest sensitivity, quantified at 1788 nm/RIU (with its equation represented as $y = 1788 \cdot x - 0.3764$). Consequently, by determining the refractive indices of brain cancer cells and utilizing the localized surface plasmon resonance (LSPR) features of this sensor, rapid detection of brain cancer cells and other pathogens becomes feasible.

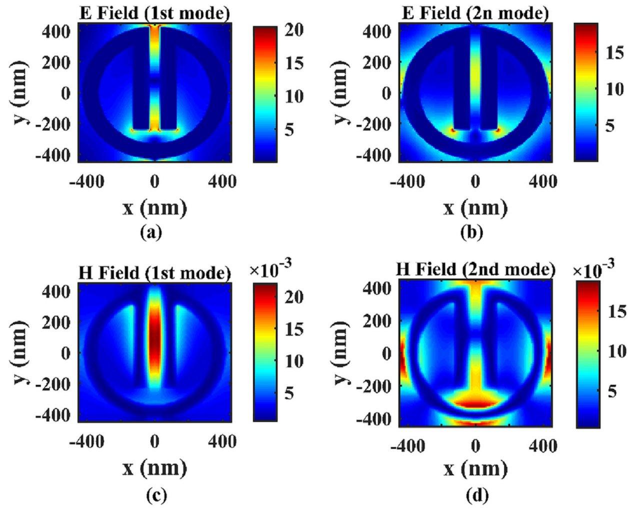

Fig. 7. (**a**,**b**) distribution of the electric field from the top view in the first and second resonance modes and, (**c**,**d**) distribution of the magnetic field from the top view in the first and second resonance modes.

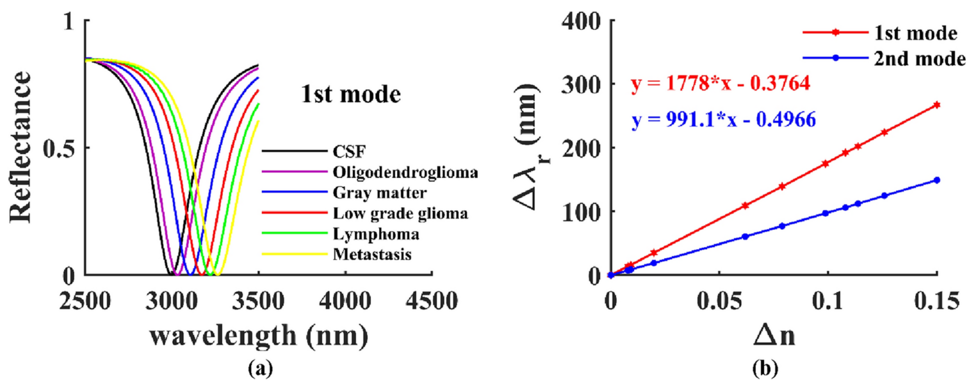

Fig. 8. (**a**) The reflectance spectrum of the sensor due to the application of different brain lesions with different refraction coefficients on the sensor measurement environment and, (**b**) the changes in resonance wavelength versus the changes in refraction coefficients due to the presence of brain lesions on the sensor measurement environment in both resonance modes in a fitting manner curve.

Impact of various conditions on system performance

As previously mentioned, the proposed structure was simulated at a polarization angle of 0°. However, for a more comprehensive analysis of our proposed sensor, we investigated the impact of the polarization angle on both TE (transverse electric) and TM (transverse magnetic) modes. As illustrated in Fig. 9a, our findings from the TE and TM polarization studies demonstrate the sensor's tunability in both single and dual resonance modes. Specifically, under TE polarization, the proposed sensor exhibits two resonance modes at wavelengths of 2990 nm and 1850 nm, corresponding to the first and second resonance modes, respectively. In contrast, under TM polarization, the system behaves as a single resonance mode at a wavelength of 1900 nm. Figure 9b further indicates that analyses conducted at various temperatures have no impact on the performance of the structure. According to the results presented in Fig. 10a, b, the same conclusion holds true regarding the angle of incident light. In other words, the proposed sensor maintains optimal performance across different temperatures and angles of incident light, demonstrating independence from these factors. This robustness in sensor performance highlights its potential applicability in various settings and conditions, making it a reliable tool for detecting biological samples such as brain cancer cells, regardless of external environmental influences.

Conclusion

This study presents an optical sensor utilizing a split-ring resonator (SRR) with a circular element, designed as a multifunctional and highly sensitive platform for the rapid, label-free, and real-time detection of brain cancer cells and other pathogens. The proposed structure was analyzed using the finite-difference time-domain (FDTD) numerical method to evaluate the minor refractive index changes caused by various biological samples, establishing it as an innovative optical sensor. The findings indicate that the designed sensor encompasses two plasmonic resonance modes in its reflection spectrum, both exhibiting high sensitivity. The first mode

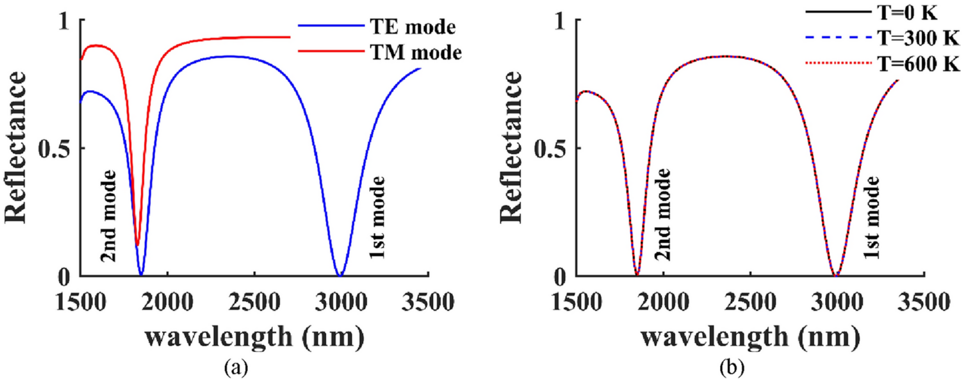

Fig. 9. (**a**) Reflectance spectrum of the sensor in TE and TM polarizations and, (**b**) reflectance spectrum of the sensor at different temperatures.

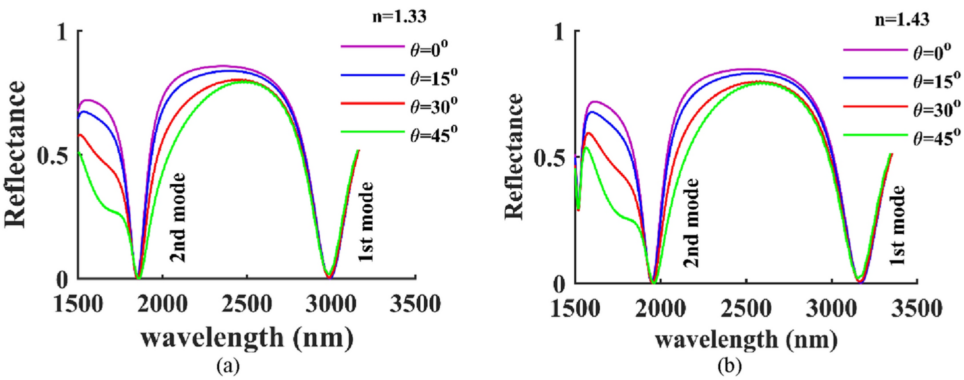

Fig. 10. (**a**,**b**) The reflectance spectrum of the proposed structure for different radiation angles in n = 1.33 and n = 1.43, respectively.

records excellent sensitivity, good limit of detection (Lod) and a commendable quality factor (QF) and figure of merit (FOM), with values of 1788.3 nm/RIU, 0.016, 11.7 and 7 RIU^{-1}, respectively. Furthermore, this study explores how geometry and metamaterials impact the sensor's performance parameters. By selecting optimal metamaterials and tuning dimensional parameters alongside the refractive index of the surrounding medium, the sensor's performance can be calibrated to distinguish between different biological samples based on its exceptional optical response. The SRR-based optical sensor features a simple, portable, and cost-effective design, delivering high sensitivity and accuracy for the rapid detection of brain cancer cells and other biological samples. The results indicate that the proposed sensor functions effectively across a broad spectrum of temperatures and angles of irradiated light, demonstrating its independence from these factors. This consistent performance highlights its potential for application in various environments, establishing it as a dependable tool for detecting biological samples, such as brain cancer cells, regardless of external conditions. This innovation holds significant potential in addressing various challenges in the development of biosensing applications, making it promising for medical, biological, and healthcare applications. SRR-based plasmonic sensors have shown considerable advancements in sensitivity and applicability for detecting biological samples; however, they frequently suffer from broad resonance curves characterized by large full width at half maximum (FWHM), resulting in low FoM that can significantly impair their detection accuracy.

Data availability
The datasets used and/or analyzed during the current study are available from the corresponding author upon reasonable request.

Received: 27 October 2024; Accepted: 26 December 2024
Published online: 02 January 2025

References
1. Perchoux, J. et al. Current developments on optical feedback interferometry as an all-optical sensor for biomedical applications. *Sensors* **16**(5), 694 (2016).
2. Mariani, S. & Minunni, M. Surface plasmon resonance applications in clinical analysis. *Anal. Bioanal. Chem.* **406**, 2303–2323 (2014).

3. Nasirifar, R., Danaie, M. & Dideban, A. Highly sensitive surface plasmon resonance sensor using perforated optical fiber for biomedical applications. *Optik* **250**, 168051 (2022).
4. Upadhyay A, Singh S, Chaudhary B, Kumar R, Singh PP, Daher M, Bhardwaj P, Eid MM, Rashed ANZ. Biosensor performance signature enhancement with silver–mxene–graphene for brain tumor diagnosis through the employment of surface plasmon resonance. *Plasmonics.* **14**, 1–12. (2024).
5. Joutsa, J. et al. Brain lesions disrupting addiction map to a common human brain circuit. *Nat. Med.* **28**(6), 1249–1255 (2022).
6. Nair V, Gimeno I, Dunn J, Zavala G, Williams SM, Reece RL, Hafner S. Neoplastic diseases. *Dis. Poult.* **14**, 548–715. (2020).
7. Monteiro, M. et al. Multiclass semantic segmentation and quantification of traumatic brain injury lesions on head CT using deep learning: an algorithm development and multicentre validation study. *Lancet Digit. Health* **2**(6), e314–e322 (2020).
8. Siddiqi, S. H. et al. Brain stimulation and brain lesions converge on common causal circuits in neuropsychiatric disease. *Nat. Hum. Behav.* **5**(12), 1707–1716 (2021).
9. Li, L. et al. Deep learning for hemorrhagic lesion detection and segmentation on brain CT images. *IEEE J. Biomed. Health Inform.* **25**(5), 1646–1659 (2020).
10. Bandyk, M. G., Gopireddy, D. R., Lall, C., Balaji, K. & Dolz, J. MRI and CT bladder segmentation from classical to deep learning based approaches: Current limitations and lessons. *Comput. Biol. Med.* **134**, 104472 (2021).
11. Karthik, R., Menaka, R., Johnson, A. & Anand, S. Neuroimaging and deep learning for brain stroke detection-A review of recent advancements and future prospects. *Comput. Methods Progr. Biomed.* **197**, 105728 (2020).
12. Khosla, A. et al. Emergence of MXene and MXene–polymer hybrid membranes as future- environmental remediation strategies. *Adv. Sci.* **9**(36), 2203527 (2022).
13 Chaudhary, V. et al. Biogenic green metal nano systems as efficient anti-cancer agents. *Environ. Res.* **229**, 115933 (2023).
14. Chaudhary, V. et al. Borophene-based nanomaterials: Promising candidates for next-generation gas/vapor chemiresistors. *J. Mater. Sci. Technol.* **218**, 236–262 (2025).
15 Chaudhary, V. A paradigm of internet-of-nano-things inspired intelligent plant pathogen-diagnostic biosensors. *ECS Sens. Plus* **1**(3), 031401 (2022).
16 Taha, B. A., Chaudhary, V., Rustagi, S. & Singh, P. Fate of Sniff-the-diseases through nanomaterials-supported optical biochip sensors. *ECS J. Solid State Sci. Technol.* **13**(4), 047004 (2024).
17. Alsalman, O. et al. Design of split ring resonator graphene metasurface sensor for efficient detection of brain tumor. *Plasmonics* **19**(1), 523–532 (2024).
18. Liu, Q. et al. Split ring resonator topology based microwave induced thermoacoustic imaging (SRR-MTAI). *IEEE Trans. Med. Imaging* **42**(8), 2425–2438 (2023).
19 Raghavan, S. Metamaterials in medicine. In *Handbook of Metamaterial-Derived Frequency Selective Surfaces* 1–20 (Springer, 2022).
20. Singh K, Dhayal M, Dwivedi S. Breast cancer detection by terahertz UWB microstrip patch antenna loaded with 6X6 SRR array. *IETE J. Res.* **70**, 1–16. (2023).
21. Singh, S., Sharma, A. K., Lohia, P., Dwivedi, D. & Singh, P. K. Design and modelling of high-performance surface plasmon resonance refractive index sensor using BaTiO3 MXene and nickel hybrid nanostructure. *Plasmonics* **17**(5), 2049–2062 (2022).
22. Gan, S., Ruan, B., Xiang, Y. & Dai, X. Highly sensitive surface plasmon resonance sensor modified with 2d ti_2c mxene for solution detection. *IEEE Sens. J.* **21**(1), 347–352 (2020).
23 Palik, E. D. *Handbook of Optical Constants of Solids* (Academic Press, 1998).
24 Nouman, W. M., Abd El-Ghany, S. S., Sallam, S. M., Dawood, A. F. B. & Aly, A. H. Biophotonic sensor for rapid detection of brain lesions using 1D photonic crystal. *Opt. Quantum Electron.* **52**(6), 287 (2020).
25. Chen, C. C. et al. Fabrication of three dimensional split ring resonators by stress-driven assembly method. *Opt. Exp.* **20**(9), 9415–9420 (2012).
26. Viskadourakis, Z. et al. Fabrication of mm-scale complementary split ring resonators, for potential application as water pollution sensors. *Materials* **16**(15), 5290 (2023).
27. Yang, K., Yao, X., Liu, B. & Ren, B. Metallic plasmonic array structures: principles, fabrications, properties, and applications. *Adv. Mater.* **33**(50), 2007988 (2021).
28. Balbinot, S., Srivastav, A. M., Vidic, J., Abdulhalim, I. & Manzano, M. Plasmonic biosensors for food control. *Trends Food Sci. Technol.* **111**, 128–140 (2021).
29. Minopoli, A., Acunzo, A., Della Ventura, B. & Velotta, R. Nanostructured surfaces as plasmonic biosensors: A review. *Adv. Mater. Interfaces* **9**(2), 2101133 (2022).
30. Rakhshani, M. R. & Mansouri-Birjandi, M. A. High sensitivity plasmonic refractive index sensing and its application for human blood group identification. *Sens. Actuators B Chem.* **249**, 168–176 (2017).
31. Mostufa, S., Paul, A. K. & Chakrabarti, K. Detection of hemoglobin in blood and urine glucose level samples using a graphene-coated SPR based biosensor. *OSA Contin.* **4**(8), 2164–2176 (2021).
32. Jalil, A. T. et al. High-sensitivity biosensor based on glass resonance PhC cavities for detection of blood component and glucose concentration in human urine. *Coatings* **11**(12), 1555 (2021).
33. Biswas, T. K. & Luu, T. In vivo MR measurement of refractive index, relative water content and T2 relaxation time of various brain lesions with clinical application to discriminate brain lesions. *Internet J. Radiol.* **13**(1), 1 (2011).
34. Gholami, A., Ahmadi-Shokouh, J. & Dashti, H. Analysis of a multi-Fano plasmonic split-ring structure using characteristic mode theory for optical applications. *Optik* **262**, 169365 (2022).
35. Khani, S. & Hayati, M. Optical sensing in single-mode filters base on surface plasmon H-shaped cavities. *Opt. Commun.* **505**, 127534 (2022).
36. Abdi, G. & Bahador, H. High sensitivity and optimum design of LSPR-based sensors by coupled nano-rings for cancer detection. *Opt. Lasers Eng.* **174**, 107975 (2024).
37. Khodaie, A. & Heidarzadeh, H. Design and analysis of a multi-modal refractive index plasmonic biosensor based on split ring resonator for detection of the various cancer cells. *Opt. Quantum Electron.* **56**(9), 1439 (2024).
38 Lulek, E., Cetin, A. E. & Ertas, Y. N. Label-free biosensing using hybrid plasmonic substrates generated via nanosphere lithography. *ACS Appl. Nano Mater.* **7**, 22793–22801 (2024).
39. Bahador, H. & Heidarzadeh, H. Highly sensitive refractive index sensor by floating nano-particles in the solution for the detection of glucose/fructose concentration. *Opt. Quantum Electron.* **53**, 1–12 (2021).
40. Danaie, M., Hajshahvaladi, L. & Ghaderpanah, E. A single-mode tunable plasmonic sensor based on an 8-shaped resonator for cancer cell detection. *Sci. Rep.* **13**(1), 13976 (2023).
41. Shahamat, Y., Ghaffarinejad, A. & Vahedi, M. Plasmon induced transparency and refractive index sensing in two nanocavities and double nanodisk resonators. *Optik* **202**, 163618 (2020).

Author contributions

All authors has same conterbition.

Declarations

Competing interests
The authors declare no competing interests.

Additional information
Correspondence and requests for materials should be addressed to H.H.

Reprints and permissions information is available at www.nature.com/reprints.

Publisher's note Springer Nature remains neutral with regard to jurisdictional claims in published maps and institutional affiliations.